

Differential expression of *miR-1*, a putative tumor suppressing microRNA, in cancer resistant and cancer susceptible mice.

Mus spretus mice are highly resistant to several types of cancer compared to *Mus musculus* mice. To determine whether differences in microRNA (miRNA) expression account for some of the differences in observed skin cancer susceptibility between the strains, we performed miRNA expression profiling of skin RNA for over 300 miRNAs. Five miRNAs, *miR-1*, *miR-124a-3*, *miR-133a*, *miR-134*, *miR-206*, were differentially expressed by both array and qPCR. *miR-1* was previously shown to have tumor suppressing abilities in multiple tumor types. We found *miR-1* expression to be lower in mouse cutaneous squamous cell carcinomas (cSCCs) compared to normal skin. Based on the literature and our expression data, we performed detailed studies on predicted *miR-1* targets and evaluated the effect of *miR-1* expression on two murine cSCC cell lines, A5 and B9. Following transfection of *miR-1*, we found decreased mRNA expression of three validated *miR-1* targets, *Met*, *Twf1* and *Ets1* and one novel target *Bag4*. Decreased expression of *Ets1* was confirmed by Western analysis and by 3' reporter luciferase assays containing wildtype and mutated *Ets1* 3'UTR. We evaluated the effect of *miR-1* on multiple tumor phenotypes including apoptosis, proliferation, cell cycle and migration. In A5 cells, expression of *miR-1* led to decreased proliferation compared to a control *miR*. *miR-1* expression also led to increased apoptosis at later time points (72 and 96 hours) and to a decrease in cells in S-phase. In summary, we identified five miRNAs with differential expression between cancer resistant and cancer susceptible mice and found that *miR-1*, a candidate tumor suppressor, has targets with defined roles in tumorigenesis.

Jessica L. Fleming^{1,†}, Dustin L. Gable^{2,†}, Somayeh Samadzadeh-Tarighat³, Luke Cheng², Lianbo Yu⁴, Jessica L. Gillespie¹, Amanda Ewart Toland^{1,5*}

¹ Department of Molecular Virology Immunology and Medical Genetics, The Ohio State University Comprehensive Cancer Center, The Ohio State University, Columbus, OH USA

² Biomedical Science Program, The Ohio State University, Columbus, OH, USA

³ Division of Hematology/Oncology, Department of Internal Medicine, The Ohio State University, Columbus, OH, USA

⁴ The Center for Biostatistics, The Ohio State University, Columbus, OH, USA

⁵ Division of Human Genetics, Department of Internal Medicine, The Ohio State University, Columbus, OH, USA

* To whom correspondence should be addressed. Amanda Ewart Toland, 460 W. 12th Avenue, Columbus, OH. Tel: +1 614 247 8185; Email: Amanda.toland@osumc.edu

† These authors contributed equally to this work.

Running title: *miR-1* in cSCC

Introduction

Mus Spretus mice are resistant to several cancer types including skin, colon, lung and thymic lymphoma (Nagase *et al.* 1995; Manenti *et al.* 1996; Villa-Morales, Santos & Fernandez-Piqueras 2006; Huang *et al.* 2007). Due to its cancer resistant nature *M. Spretus* has been used for quantitative trait locus (QTL) mapping for cancer susceptibility loci (Dejager, Libert & Montaguettli 2009). To date, most of the QTL studies for cancer susceptibility have focused on identification of candidate genes with amino acid substitutions or differences in mRNA expression. Recent genome-wide association studies for cancer risk in humans have identified cancer-associated polymorphisms with roles in regulation of gene expression (Pomerantz *et al.* 2009; Spain *et al.* 2012).

MicroRNAs (miRNAs) are short RNAs of 20-22 nucleotides with well-documented roles in gene regulation (Siomi & Siomi 2010). They bind to the 3'untranslated region (3'UTR) of genes and may be involved in binding to other parts of the mRNA as well (Wery, Kwapisz & Morillon 2011). Binding results in mRNA degradation or impaired translation and subsequent decreased protein expression (Shyu, Wilkinson & van Hoof 2008; Djuranovic, Nahvi & Green 2011). Increasing evidence indicates that miRNAs play key roles in carcinogenesis. Expression profiling studies have demonstrated that many miRNAs are down-regulated during tumor development, resulting in subsequent up-regulation of their target genes and respective proteins. These miRNAs act as tumor suppressors and target cell cycle, apoptosis, proliferation, invasion and metastasis genes (Croce 2009). Likewise, another subset of miRNAs is up-regulated during

tumorigenesis resulting in down-regulation of their targets which are frequently tumor suppressor genes (Medina & Slack 2008). Previous studies indicate that several miRNAs map in close proximity to mouse QTLs for cancer susceptibility suggesting that variations in miRNA sequence or expression may be important for cancer susceptibility (Sevignani *et al.* 2007).

Because of the strong correlation between miRNA expression and tumorigenesis, we hypothesized that miRNAs showing differential expression between skin cancer resistant *M. spretus* (SPRET/EiJ) mice and skin cancer susceptible *M. musculus* (FVB/NJ) mice could be considered as candidates for cancer susceptibility. To identify miRNAs which may play a role in differences in cancer susceptibility between SPRET/EiJ and FVB/NJ, we performed expression profiling on normal skin samples from these strains of mice. Five differentially expressed miRNAs with described roles in tumorigenesis were identified and validated. Based on our observations and reports in the literature supporting *miR-1* as having tumor suppressor function in a variety of cancer types (Nasser *et al.* 2008; Datta *et al.* 2008; Yan *et al.* 2009; Li *et al.* 2012; Hudson *et al.* 2012; Nohata *et al.* 2011; Nohata *et al.* 2012a; Nohata *et al.* 2012b; Tominaga *et al.* 2013), we hypothesized that *miR-1* acts as a tumor suppressor in cutaneous squamous cell carcinoma (cSCC). Here, we describe the effects of expressing *miR-1* in cSCC cells and the identification of Ets1, as a *miR-1* target in the mouse.

Materials and Methods

RNA isolation

Animal studies were approved by the Ohio State University (OSU) and University of California, San Francisco Institutional Animal Care and Use Committees. The OSU IACUC determined that the research performed at OSU was exempt from IACUC review as pre-existing or commercially available animal specimens were used for this study. Fresh frozen skin samples from three FVB/NJ and three SPRET/EiJ female mice aged 4-5 weeks were obtained through the Jackson Laboratory surgical service. RNA was isolated from the skin using standard Trizol extractions (Invitrogen, Grand Island, NY). We isolated RNA a second time from two of the skin samples to generate a replicate control for the microarrays. Samples were DNAase treated. RNA was quantitated using Nanodrop (ThermoScientific, Wilmington, DE). RNA was isolated from eleven cSCCs from chemically treated C57Bl6/FVB F1 mice using standard Trizol methods. RNA samples were DNAase treated.

MicroRNA expression arrays and data analysis

Five μ g of total RNA from each sample was sent to the OSU Comprehensive Cancer Center MicroArray Shared Resource for miRNA expression analysis using the miRNA microarray chip OSUCCC version 4.0 (Liu *et al.* 2004; Liu *et al.* 2008). For each strain of mice, a fourth RNA sample of a second independent RNA isolation was also evaluated. The arrays contain over 300 human and mouse miRNAs spotted in triplicate with probes for both precursor and mature miRNAs. Experiments were performed and analyzed as previously described (Liu *et al.* 2004; Liu *et al.* 2008). In brief, a linear model was employed to detect differentially expressed miRNAs. In order to improve the

estimates of variability and statistical tests for differential expression, a variance smoothing method with fully moderated t-statistic was employed for this study (Yu *et al.* 2011). The significance level was adjusted by controlling the mean number of false positives (Gordon *et al.* 2007).

Quantitative PCR

Quantitative PCR (qPCR) validation of candidate miRNAs. qPCR was performed using Applied Biosystems Taqman probes to validate expression of the six candidate miRNAs (Foster City, CA). Probes were specific to either mature (*miR-1*, *miR-133a*, *miR-124a-3*, *miR-206*) or precursor (*miR-134*, *miR-206*, *miR-9-1*) miRNAs concordant with the array results. Reverse transcription for mature miRNAs was performed using Applied Biosystem's High Capacity cDNA Reverse Transcription reagents according to manufacturer's protocol in 7.5 µl reactions (Carlsbad, CA). Three independent skin RNA samples were used for each strain from samples not used on the original arrays. qPCR of *miR-1* levels from eleven primary mouse cSCCs was conducted as for normal skin. For miRNA quantification, real-time PCR was performed using Applied Biosystem Taqman Assays per manufacturer's recommended conditions. All samples were done in triplicate. qPCR runs included no template and no-reverse transcriptase controls. Expression was normalized to expression levels for *sno202* RNA for mature miRNAs or to *L19* for pri-miRNAs. qPCR was conducted using Applied Biosystems 7900HT instrument. Cycle threshold (CT) values were averaged across triplicates and delta CT values were calculated between each test miRNA and control. The fold expression of SPRET/EiJ miRNA relative to FVB/NJ was calculated. Standard deviations of fold

differences of the percentage of reference gene expression were made by comparisons between independent RNA samples of each of the test samples. Student's t-test was used to calculate p-values for the qPCR. A nonparametric Mann-Whitney U test was performed to test for differences between in *miR-1* expression in tumors versus SPRET/EiJ and FVB normal skin .

qPCR of predicted mRNA targets. To measure expression of predicted targets, mRNA expression was measured at 48 and 72 hours post *miR-1* or scrambled precursor miR negative control transfection in A5 cells and at 48, 72 and 96 hours post-transfection in B9 cells using SYBR green quantitative real-time PCR. Reverse transcription of mRNA was performed using a Bio-Rad iScript cDNA synthesis kit according to manufacturer's recommended conditions. Primers were designed using Integrated DNA Technologies. Target gene expression was measured using Bio-Rad SYBR Green Supermix in 10 µl reactions according to manufacturer's protocol. qPCR of each sample was performed in triplicate and was used to measure *Ets1*, *Met*, *Bag4*, *Twf1*, *Sp1*, *Taok1*, *Zfp148* and *Trp53* target gene expression. The following primer sets were used. *Ets1*: Forward: 5' TGTATGAGTGGAGCAGCACTGTGT 3', Reverse: 5' AGGTAGGGTCTCCATTAACCT 3', *Met*: Forward: 5' AACGGGTATTGGGAAGACCCTGAA 3', Reverse: 5' ATCCCGTCTAACAGGAAGAAGGCT 3', *Bag4*: Forward: 5' ACTCCACGGAAGTTCCAA ACACCT 3', Reverse: 5' TTCCAGGGTTCTGTGAAGCAGGAT 3', *Twf1/Ptk9*: Forward 5' TTCCAGGCTTTGGAGAAGGTGAGT 3', Reverse: 5' AGTCTCCTTCGTGGGAATGCTTGT 3', *Sp1*: Forward 5'

137 TCGGGCAAAGTATATGGCAAGACC 3', Reverse 5'

138 ACTCCTCATGAAACGCTTAGGGCA 3'

139 *Taok1*: Forward 5' GAACCAGGCCAAGTGAAACTTGCT 3', Reverse 5'

140 AAAGGAGGCTTCCTCTCGGCTAAT 3'

141 *Zfp148*: Forward 5' GCACTGCAATGCTGCCTTTAGAAC 3', Reverse 5'

142 TTTGCGCCGGTATGGATCTTCTCGT 3'

143 *Trp53*: Forward 5' ACAAGAAGTCACAGCACATGACGG 3', Reverse 5'

144 TTCCTTCCACCCGGATAAGATGCT 3'

145 and *L19*: Forward: 5' ATTCCCGGGCTCGTTGCCGGAAAA 3', Reverse: 5'

146 ATTGGCAGTACCCTTCCTCTTCCCTA 3'. Candidate targets were normalized to *L19*

147 expression and fold difference relative to the scrambled control at 48 hours post-

148 transfection were calculated. Standard deviations of fold differences of the percentage

149 of reference gene expression were made by comparisons between independent RNA

150 samples. Experiments included no template and no reverse transcriptase controls for

151 each gene. Student's t-test was used to calculate p-values.

152

153 *qPCR confirmation of transfections*. RNA was isolated from a duplicate well for each

154 mock, scrambled control or *miR-1* transfected experiment to confirm increased *miR-1*

155 expression in the *miR-1* transfected cells. qPCR for *miR-1* expression was conducted

156 as described above.

157

158 ***Identification of candidate target genes for differentially expressed microRNAs***

Target prediction programs, www.microRNA.org (Beta *et al.* 2008) and www.targetscan.org were searched for predicted mRNA targets for *miR-1* in both mouse and human. Targets for *miR-1* were prioritized for further study by the number of predicted binding sites per 3'UTR (> 1 site), strength of binding score, and predicted binding of the miRNA in both human and mouse. A literature scan was also performed to identify targets which had previously been validated experimentally.

Cell culture and transient transfections

A5 and B9, mouse cutaneous spindle and cSCC cell lines respectively, and C5N, a non-tumorigenic mouse keratinocyte cell line, were used for these studies (Zoumpourlis *et al.* 2003). Cell lines were grown in Dulbecco's medium supplemented with 10% fetal bovine serum and 1% penicillin/streptomycin in an atmosphere of 5% CO₂. Transient transfections were performed using Invitrogen Lipofectamine 2000 according to manufacturer's protocol (Life Technologies, Grand Island, NY). Mock and negative control (scrambled pre-miR) transfections were carried out for all experiments when cells were at 40-50% confluency. Scrambled pre-miR (AM17110) negative control and *miR-1* (AM17150) precursor were purchased from Ambion (Life Technologies, Grand Island, NY).

Western blot analysis

Protein from whole cell extracts was extracted 24, 48, 72 and 96 hours post-transfection via solubilization of A5 and B9 cells using RIPA buffer (50 mM Tris base pH 8, 150 mM NaCl, 1% NP40, 0.10% SDS) containing a protease inhibitor (Roche). For each

sample, 30 μ g of protein were run on a 10% polyacrylamide gel in a Bio-Rad mini-gel system at 150V (12V/cm) for ~1.5 hours. Proteins were transferred to nitrocellulose membrane for 70 minutes at 90V (7V/cm). Following transfer, membranes were blocked in 5% milk in TBST (10X TBS: 1.2% Tris, 8.8% NaCl) and were incubated with primary antibody overnight. Antibodies and dilutions were as follows: Ets1, 1:1000 dilution (antibody a gift from Michael Ostrowski) and α -tubulin, 1:100 dilution (T5168, Sigma-Aldrich, St. Louis, MO). Incubation with secondary antibodies was for 2 hours. Secondary antibodies and dilutions were as follows: Anti-mouse HRP-Linked, 1:10000 dilution (W4021, Promega, Madison, WI), Anti-Rabbit HRP-Linked Antibody, 1:1000 dilution, (7074S, Cell Signaling Technology, Danvers, MA). Enhanced chemiluminescent reagent (Thermo Scientific, Rockford, IL) was applied in a 1:1 ratio.

Luciferase Assays

Cloning. Cloning of *Ets1* 3'UTR was performed using In-Fusion Advantage PCR Cloning Kit according to manufacturer's protocol (Clontech Mountain View, CA). Full length *Ets1* plasmid with 3'UTR provided by Dr. Michael Ostrowski was used as a template for PCR. A 1,278 base pair product was generated containing the predicted three *miR-1* binding sites and was cloned into a pGL3 Control Luciferase vector (Promega, Madison, WI). Primers used for cloning were as follows: *Ets1* 3' UTR In-Fusion Forward: 5'-tgtaatactagtagccgAGAAGAGAGGCAATTGGCTGAGGT-3', *Ets1* 3' UTR In-Fusion Reverse: 5'-gtctgctcgaagcggACTGAGGCAGTATTCCTGATAGAG-3'. Clones were sequence verified. Site-directed mutagenesis was carried out to mutate two base pairs in each of the three *miR-1* binding sites in the *Ets1* 3'UTR using QuikChange Lightning

Multi Site-Directed Mutagenesis kit according to the manufacturer's protocol (Agilent Technologies, Santa Clara, CA). Primers used for site-direct mutagenesis are as follows:

Ets1 3' UTR SDM 1 Forward: 5'-gttgatggctgactcccactctccctgaagactctgaat-3',

Ets1 3' UTR SDM-1 Reverse: 5'-attcagagcttcaagggagagtgaggagtcagccatcaac-3',

Ets1 3' UTR SDM-2 Forward: 5'-ccacaaggaagcaaaggccaaactctccagctatatatatttgatctta-3' ,

Ets1 3' UTR SDM-2 Reverse: 5'-taagatcaaaatatatagctggagagtttggcctttgcttccttgagg-3',

Ets1 3' UTR SDM-3 Forward: 5'-acctgttgaaactcttacgtactctccaaagacgtttcaaggaac-3',

Ets1 3' UTR SDM-3 Reverse: 5'-gttccttgaaacgtctttggagagtagtaagagttcaacaggt-3'.

Clones were sequenced verified.

Transfections and luciferase assays. C5N and A5 cells were plated in triplicate into a 12-well dish at 24 hours prior to transfection. At 70% confluency, 0.10 µg Luc-*Ets1* 3'UTR and Luc-*Ets1* 3'UTR-mutated were each co-transfected with 10 pmol of a scrambled control miR or *miR-1* into each well. 0.10 µg of a PRL-TK vector (TK-driven *Renilla* luciferase vector, Promega) was also transfected into each well to normalize the firefly luciferase values. All experiments included mock and pGL3-Control empty vector controls. A5 and C5N cell lysates were prepared using M-PER (Pierce Biotechnology, Rockford, IL) and 30 µg of each sample were used for analysis. Firefly and renilla luciferase measurements were acquired 24 hours post-transfection using a Veritas Microplate Luminometer.

Cell proliferation assay

At 24 hours post-transfection with *miR-1*, scrambled miR control or mock transfected, A5 and B9 cells were trypsinized and 2000 cells (A5) or 3000 cells (B9) were plated in quadruplicate in a 96-well plate. Proliferation was measured at 24, 48, 72 and 96 hour post-transfection using a MTT ((3-(4,5-Dimethylthiazol-2-yl)-2,5-diphenyltetrazolium bromide) cell proliferation kit (Roche, Indianapolis, IN). Experiments were carried out according to manufacturer's protocol. RNA and protein were isolated at each solubilization step. Optimal absorbance of the formazan product was measured at wavelength of 550 nm and a reference wavelength of 690 nm was used. For each sample, absorbance was normalized to the reference wavelength as well as a blank control, which contained media only.

Cell cycle assay

A5 and B9 cells were transfected with *miR-1*, scrambled miR control or mock transfected. Cells were trypsinized and counted 48, 72 and 96 hours post-transfection. Two million cells were fixed in 70% ethanol. Cell cycle analysis was evaluated by DNA content. Cells were incubated with a propidium iodide solution (0.1% Triton X-100, 0.2 mg/mL DNase-free RNase A and 20 µg/mL propidium iodide for 15 minutes at 37°C (B9 cells) or 30 minutes at 20°C (A5 cells). Data was acquired on a BD FACS Calibur instrument. ModFit software was used for analysis. Experiments were done in triplicate.

Apoptosis assay

A5 and B9 cells transfected with *miR-1* or scrambled miR control were trypsinized and counted at 48, 72 and 96 hours post-transfection. The FITC Annexin V Apoptosis Detection Kit I was used to evaluate cell death according to manufacturer's protocol (BD Biosciences, San Jose, CA). Unstained, FITC Annexin only, and propidium iodide only conditions were used as controls. Data was acquired on a BD FACS Calibur instrument. Cell Quest Pro for was used for data analysis. Experiments were done in triplicate.

Cell motility assay

A5 and B9 cells were plated at a density of 7×10^5 cells/mL in ibidi cell culture inserts according to the manufacturer's protocol (Martinsried, Germany) at approximately 48, 72 and 96 hours post-transfection. Transfections of A5 and B9 cells included mock transfection, scrambled miR control (AM17110) or *miR-1* precursor (AM17150) as described above. Eight hours after plating, cell inserts were removed. Images were taken at 5X magnification using AxioVision 4.8 software on an Axiovert 25 microscope at 0 hours and every 5-8 hours until gaps closed. Images were assessed visually by two independent researchers for differences in rate of gap closure.

Results

miRNA profiling of normal skin of cancer resistant and cancer susceptible mice

We hypothesized that miRNAs differentially expressed between cancer resistant and cancer susceptible mice might have oncogenic- or tumor suppressor-like properties in the skin. To identify miRNAs that were differentially expressed between cancer resistant SPRET/EiJ and cancer susceptible FVB/NJ mice, we performed miRNA

expression profiling of total RNA isolated from four normal skin samples per strain. The miRNA arrays contained probes for precursor and mature miRNAs of approximately 300 miRNAs (Supplementary Table S1; Liu *et al.* 2004; Liu *et al.* 2008). Following analysis, six miRNAs (*miR-1*, *miR-133a*, *miR-124a-3*, *miR-134*, *miR-206*, and *miR-9-1*) showed a significant difference in average expression and had a 2.0 fold or greater difference across one or more probe sets. All of these showed higher expression in SPRET/EiJ (Table 1). Due to the evolutionary divergence between *M. musculus*, for whom the majority of arrays have been designed, and *M. spretus*, lower miRNA expression observed in SPRET/EiJ mice could indicate a sequence polymorphism. However, we observed the opposite effect in which all miRNAs showing differential expression were higher in SPRET/EiJ; these results decrease the likelihood that the observed profiles were due to polymorphic variants between the strains.

To validate the expression differences of the six miRNAs showing differential expression between SPRET/EiJ and FVB/NJ by microarray, we performed qPCR using Applied Biosystems Taqman probes on samples from mice not used in the initial array studies. Probes were specific to either mature (*miR-1*, *miR-133a*, *miR-124a-3*, *miR-206*) or precursor (*miR-9*, *miR-134*, *miR-206*) miRNAs and were chosen for evaluation based on the specific probe sets (mature versus precursor) that showed differences by microarray (Table 1). Five of the six miRNAs evaluated showed similar fold-differences in expression between microarray and qPCR for FVB/NJ and SPRET/EiJ skin (Figure 1 and data not shown); however, only *miR-1*, *miR-133a* and *miR-206* showed statistically significant differences in expression by qPCR (p-value < 0.05).

***miRNA-1* expression decreased in mouse cSCCs**

We hypothesized that miRNAs expressed at higher levels in SPRET/EiJ mice relative to FVB/NJ mice would behave similarly to tumor suppressor genes and exhibit reduced expression in tumors. We chose *miR-1* for expression studies in mouse cSCCs to test our hypothesis because it showed significant difference in expression between FVB/NJ and SPRET/EiJ for six probes on the array and showed a significant difference in expression by qPCR (Table 1). In addition, there was evidence from the literature showing down-regulation of *miR-1* in a variety of human cancers and a link between *miR-1* down-regulation and cancer phenotypes (Nasser *et al.* 2008; Datta *et al.* 2008; Yan *et al.* 2009; Nohata *et al.* 2012a; Nohata *et al.* 2012b). From these data, we expected that *miR-1* expression would be decreased in mouse cSCCs. To evaluate *miR-1* expression in cSCC, we performed qPCR of *miR-1* in eleven cSCCs isolated from DMBA/TPA chemically-treated C57Bl6/FVB mice. The median *miR-1* expression was lower in the tumors (3% of control *sno-202*) compared to median *miR-1* expression in FVB/NJ (22% of control *sno-202*) and SPRET/EiJ (110 of control *sno-202*). The difference in expression was significant between the tumors and SPRET/EiJ (Figure 2, p-value=0.012). Based on the expression data in the primary tumors and the strain specific differences in expression, we chose *miR-1* as a strong candidate miRNA to evaluate further for a role in cSCC.

qPCR of miR-1 candidate target genes

miRNAs are thought to impact gene regulation by targeting mRNAs for degradation via complete sequence matches or inhibition of translation when there is imperfect binding between a miRNA and its target sequence (Djuranovic, Nahvi & Green 2011). We hypothesized that if the difference in miRNA expression between the strains of mice was important in cancer susceptibility there would be differences in target mRNA expression of genes associated with carcinogenesis. To identify putative targets of *miR-1*, *miR-133a*, *miR-124a-3*, *miR-134*, and *miR-206*, we searched the literature to identify targets of these miRNAs that had been detected by expression arrays in tumors and had been further validated by other methods. We also identified genes predicted to be targets in microRNA databases www.microRNA.org (Beta *et al.* 2008) and www.targetscan.org. We prioritized genes as candidates which had two or more predicted binding sites, had stronger binding scores and those genes previously implicated in cancer. Using these strategies, we identified multiple candidate targets for each miRNA (Supplemental Table S2).

We chose seven putative *miR-1* targets, *Bag4*, *Ets1*, *Met*, *Sp1*, *Taok1*, *Trp53*, and *Zfp148*, and one positive control, *Twf1*, which previously had been shown to be a *miR-1* target by Applied Biosystems, for testing. These candidate target genes were prioritized based on our database searches and those which had been validated in the literature as being targets of *miR-1* in studies of primary human tumors or cancer cell lines. By qPCR, two of the candidate targets, *Ets1* and *Met*, and our positive control *Twf1* showed significant down-regulation in *miR-1* transfected A5 cells compared to scrambled miR precursor transfected cells at both 48 and 72 hours post-transfection

(Figure 3 and Supplemental Figure S1, *Met* p-values 0.0001 and 0.002; *Ets1* p-value=0.0001 and 0.0002; *Twf1* p-values=0.0001 and 0.006 respectively). Our positive control, *Twf1*, showed decreased expression in *miR-1* transfected B9 cells at 48, 72 and 96 hours (p-values=0.0004, 0.0002 and 0.03 respectively). In B9 *miR-1* transfected cells *Met* showed significantly decreased expression only at 48 hours (p-value=0.001), and *Ets1* showed significantly decreased expression at 48 and 72 hours post-transfection compared to scramble miR control transfected cells (p-values 0.008 and 0.005 respectively). *Bag4* mRNA expression was significantly reduced in B9 cells transfected with *miR-1* at all three time points (Supplemental Figure S1; 48 hour p-value=0.0007, 72 hour p-value=0.02 and 96 hour p-value=0.004), but it only showed significant down-regulation of mRNA at 72 hours in A5 cells transfected with *miR-1* compared to scrambled control cells (Figure 3D and Supplemental Figure S1, p-value=0.01). The remaining targets did not show statistically significant differences in expression between control and *miR-1* A5 transfected cells (data not shown).

Evaluation of Ets1 as a miR-1 target

mRNA expression data is only correlative and does not show a direct effect of miRNAs on predicted target gene expression. As *Ets1* had not been confirmed as a target of *miR-1* in the mouse, and since several studies support a role of *Ets1* in cSCC and cancer phenotypes such as metastasis, apoptosis and proliferation, we decided to further evaluate murine *Ets1* as a *miR-1* target (Keehn, Smoller & Morgan 2004; Hahne *et al.* 2009; Nagarajan *et al.* 2009). We first assessed whether *Ets1* protein levels were decreased by *miR-1* expression. By Western, *Ets1* was down-regulated in the *miR-1*

transfected A5 cells at 24, 48 and 72 hours post-transfection and in B9 cells at 48 and 96 hours post-transfection compared to scramble control miR transfected cells (Figure 4a and 4b; Supplemental Figure S2). As this could be an indirect effect of *miR-1* expression, we assessed the effect of *miR-1* expression on a luciferase construct containing the 3'UTR of *Ets1*. *miR-1* expression resulted in lower luciferase expression with the wildtype *Ets1* 3'UTR compared to a scrambled precursor miRNA. Furthermore a construct containing mutated *miR-1* binding sites did not show reduced luciferase expression providing additional evidence that *miR-1* regulates *Ets1* expression via direct binding to the predicted *miR-1* binding sites in the *Ets1* 3'UTR (Figure 4c). Our data is consistent with a publication showing *Ets1* to be a target of *miR-1* in a human liver cancer cell line (Wei *et al.* 2012).

Functional characterization of miR-1 expression

***miR-1* expression in cSCC cells decreases cell proliferation**

There are several published studies showing *in vitro* and *in vivo* effects of *miR-1* on tumor suppression (Nasser *et al.* 2008; Datta *et al.* 2008; Yan *et al.* 2009; Nohata *et al.* 2011, Nohata *et al.* 2012a, Nohata *et al.* 2012b). Based on these, we anticipated that expression of *miR-1* in cSCC cells would have tumor suppressing abilities (Nohata *et al.* 2012b). To determine if *miR-1* decreased cell proliferation, we transfected A5 and B9 cSCC cells with *miR-1* or scrambled precursor miRNA. Cell proliferation was measured by an MTT assay at 24, 48, 72 and 96 hours post-transfection. We observed a significant decrease of 1.7-fold in absorbance at 96 hours post-transfection in A5 *miR-1* transfected cells compared to the scrambled control miR transfected cells suggesting

that *miR-1* is playing a role in growth inhibition (Figure 5a, 72 hour p-value=0.01; 96 hour p-value=0.0001). A modest, but significant decrease in proliferation was observed at the 72 hour time point in the B9 cSCC cell line, but there was no difference in proliferation at 96 hours (Figure 5b, 72 hour p-value=0.02; 96 hour p-value=0.3).

The effect of miR-1 expression on additional tumor phenotypes

miR-1 has been shown to induce apoptosis in multiple cancer cell lines including maxillary sinus SCC, head and neck SCC, and renal cell carcinoma (Nohata *et al.* 2011; Kawakami *et al.* 2011; Nohata *et al.* 2012a; Nohata *et al.* 2012b). To determine if the decreased proliferation seen in the cells transfected with *miR-1* was the result of increased apoptosis, we performed FACS analysis of AnnexinV and PI stained *miR-1* transfected and scramble control miR transfected A5 and B9 cells. No significant differences in apoptosis were observed at 48 or 72 hours post-transfection in the A5 cells; however, there was a significant increase in apoptosis at 96 hours (p-value=0.036; Figure 6a, Supplemental Figure S3). The B9 cells showed a statistically significant decrease in apoptosis in the *miR-1* transfected cells at 48 hours (p-value=0.04) and a statistically significant increase in apoptosis at 72 hours (p-value=0.003). There were no differences in apoptosis at 96 hours (Figure 6b, Supplemental Figure S3). The apoptosis data for the A5 and B9 cell lines are consistent with the proliferation results.

Ectopic expression of *miR-1* has also been shown to induce G0/G1 arrest in several different cancer cell lines (Nohata *et al.* 2012b). We evaluated cell cycle parameters in *miR-1* transfected cells by FACS analysis (Figure 6, Supplemental Figure S4). We

observed modest but consistent and statistically significant fewer cells in the S phase for *miR-1* transfected A5 cells compared to scrambled control miR transfected A5 cells at 48, 72, and 96 hours (p-values=0.002, 0.0001 and 0.006 respectively, Figure 6C, 6E, 6G) and for *miR-1* transfected B9 cells at 48 and 96 hours (p-values=0.001 and 0.007 respectively, Figure 6D and 6H). There was a trend for a modest increase in cells in G0/G1 for *miR-1* transfected A5 cells at all time points, but this was only significant at 48 hours post-transfection (p-value=0.04; Figure 6C). This was not observed in the B9 cells. There was a trend for more cells in G2-M in the *miR-1* transfected cells for both A5 and B9 for some time points (Figure 6, Supplemental Figure S4), but the absolute differences are quite small and were not significant except for the *miR-1* transfected B9 cells at 48 hours (p-value=0.02, Figure 6F). These results suggest that *miR-1* may have an extremely modest effect on cell cycle progression resulting in fewer cells in S phase.

Previous studies have reported a role of *miR-1* in migration. In addition, Ets1 has a well-documented role in enhancement of migration (Hahne *et al.* 2005; Smith *et al.* 2012). To test whether *miR-1* affects migration in cSCC, we performed cell motility assays of *miR-1* transfected and scrambled control transfected A5 and B9 cells at approximately 24, 48, 72 and 96 hours post-transfection. No consistent differences were observed in cell motility between *miR-1* and scrambled control miR transfected cells for any of the time points (Figure 7, Supplemental Figure S5 and data not shown). Closure of gap appeared to be directly proportional to gap width.

miR-1 expression following transfection was confirmed for all phenotypic experiments by qPCR and is below detectable limits for the mock or scrambled control transfected A5 and B9 cell lines.

Discussion

Exploitation of genetic differences between cancer resistant and cancer susceptible mice has led to the identification of candidate genes important in tumorigenesis, but little has been explored regarding the differences in miRNA expression profiles in these mice. Here, we describe our discovery of five miRNAs showing higher expression in skin cancer resistant mice compared to skin cancer susceptible mice. In more detailed analyses of one miRNA, *miR-1*, we show that *miR-1* expression leads to decreased cell proliferation which may be the result of modestly higher apoptosis in later time points (72 or 96 hours) in combination with a reduced number of cells in S phase. We also observed decreased mRNA expression of previously described human *miR-1* targets, *Met*, *Twf1*, and *Ets1*, in the mouse which establishes that *miR-1* targets these mRNAs in more than one species. Furthermore, we show that *Bag4*, a novel *miR-1* target, is significantly down-regulated in the B9 cell line.

miR-1, *miR-133a*, and *miR-206* are all part of a group of myo-miRs, miRNAs whose expression is enriched in skeletal and cardiac muscle (McCarthy 2008). All three of these miRNAs showed higher expression in cancer resistant SPRET/EiJ compared to FVB/NJ normal skin. Initial studies on *miR-1* focused on its expression in heart and skeletal muscle as it was thought not to be expressed in other tissues. In

cardiomyocytes *miR-1* regulates apoptosis via Bcl-2 and IGF-1 (Yu *et al.* 2008; Tang *et al.* 2009). In skeletal muscle, *miR-1* has a role in cellular proliferation and differentiation (Chen *et al.* 2006). All of these functions are also important in tumorigenesis and are consistent with a role for *miR-1* in cancer. A connection between expression of myo-miRs and skin cancer susceptibility has previously been made; a gene network for skin cancer susceptibility from the same strains of mice studied here was found to be enriched in muscle related mRNAs (Quigley *et al.* 2009).

Decreased *miR-1* expression has been observed in a number of cancers including skin, lung, liver, bladder, renal and prostate (Li *et al.* 2012; Hudson *et al.* 2012; Nohata *et al.* 2012a; Tominaga *et al.* 2013; Nohata *et al.* 2012b). This is not the first study to look at the role of *miR-1* in the skin or in SCCs. By array analysis, *miR-1* showed about a 2-fold down regulation in human cSCCs compared to matched normal skin (Darido *et al.* 2011). *miR-1*, along with *miR-133a*, *miR-205* and *let-7d*, shows decreased expression in SCCs of the head and neck in comparison to normal adjacent tissue (Childs *et al.* 2009). Consistent with their down-regulation in tumors, numerous studies have demonstrated tumor suppressor functions of *miR-1*. Increased expression of *miR-1 in vitro* has been associated with increased apoptosis, decreased migration and decreased cell growth (Hudson *et al.* 2012; Wei *et al.* 2012; Yamasaki *et al.* 2012; Yoshino *et al.* 2012). *miR-1* was also found to target c-Met in rhabdomyosarcomas and colorectal cancer leading to decreased cell motility and proliferation (Yan *et al.* 2009; Reid *et al.* 2012). Our results showed decreased *Met* mRNA expression in cells transfected with *miR-1*, but observed no correlation between *miR-1* expression and cell

motility. In this study, we identified a correlation with proliferation and *miR-1* expression levels which is consistent with other studies (Yan *et al.* 2009; Reid *et al.* 2012).

In contrast to previous studies we observed only modest effects of *miR-1* on apoptosis and cell cycle and did not observe any consistent effects on migration. We observed a consistent decrease in the percentage of *miR-1* transfected cells in S phase and a non-significant increase of *miR-1* transfected cells at G2/M compared to scrambled control cells for some time points, but these differences were very modest compared to studies by others (Nohata *et al.* 2011; Hudson *et al.* 2012; Kawakami *et al.* 2012; Wei *et al.* 2012). We also observed increases in apoptosis in both B9 and A5 cells transfected with *miR-1*, but the apoptosis was only observed at later time points and the percentage of cells undergoing apoptosis was less compared to other studies (Hudson *et al.* 2012; Wei *et al.* 2012; Yoshina *et al.* 2012). Finally, we observed no significant differences in cell motility of *miR-1* transfected A5 or B9 cells. There are several potential explanations for the observed results. First, these cell lines may not be as responsive to the effects of *miR-1* because they do not express high levels of other pro-tumorigenic *miR-1* targets not studied here. Some *miR-1* oncogene-like targets have been identified that were not evaluated for expression in our cells. However, many of the targets tested in our study that have been reported to have oncogenic properties, such as *Bag4*, *Ets1* and *Met*, showed decreased expression in A5 and/or B9 cells following *miR-1* transfection. Another possible explanation for the discordant results is that we evaluated the effects of *miR-1* expression in mouse and not human cell lines. Most of the published studies on *miR-1* have been in human cancers and using human cell lines and it is possible that

miR-1 has unique targets in the mouse which confer tumor suppressor activities that ameliorate some of the effects of silencing target oncogenes. Additional studies are warranted to further explore these and other possibilities.

Ets1 is a transcription factor that has been described as a proto-oncogene due to its pro-tumorigenic effects and its discovery in chickens affected with the avian erythroblastosis virus, E26 (Dittmer 2003). Specifically, Ets1 has been shown to play a role in cSCC tumor development and progression (Pande *et al.* 1999; Nagarajan *et al.* 2009). Ets1 acts as a cSCC tumor promoting gene by inducing cSCC cell proliferation in transgenic mice over-expressing Ets1 (Pande *et al.* 1999). Studies show that Ets1 regulates genes important in apoptosis, angiogenesis, migration, invasion, and matrix metalloproteinases which enhance cell migration (Pande *et al.* 1999; Keehn, Smoller & Morgan 2004; Hahne *et al.* 2005). In addition, it is over-expressed in human cSCC malignancies (Keehn, Smoller & Morgan 2004; Saeki *et al.* 2000; Saeki *et al.* 2002). A previous study looked at Ets1 expression in 26 primary skin lesions. Ets1 nuclear expression was present in cSCC in situ, but was the highest in poorly differentiated or metastatic cSCCs (Keehn, Smoller & Morgan 2004). These results suggest the importance of dysregulation of Ets1 expression for progression of cSCC. Consistent with a role for *miR-1* in dysregulation of Ets1 in cancer, a study published after we chose Ets1 as a candidate showed that Ets1 is targeted by *miR-1* in HepG2 cells (Wei *et al.* 2012). Ets1 is involved in regulation of numerous protein tyrosine kinases (PTKs), a class of molecules to which a majority of known oncogenes belong (Hahne *et al.* 2009). Some predicted Ets1 targets include EGFR, FGFR4, INSR, MET, PDGFRA, and

VEGFR1 (Hahne *et al.* 2009). Ets1 has been shown to be involved in regulation of tumorigenesis by promotion of the EGFR-Ras-MEK1/2 MAPK pathway (Roberts & Der 2007; Ciardiello & Tortora 2008; Montagut & Settleman 2009; Knight, Lin & Shokat 2010). Our positive control for *miR-1* transfection, *Twf1*, also belongs to the family of PTKs regulated by Ets1. As *miR-1* has multiple experimentally validated targets from this study (*Ets1*, *Met*, *Bag4*) and from published studies (MET, PTK1, HDAC4, ANXA2, BDNF and FOXP1) that have roles in tumorigenesis, it is likely that *miR-1*'s ability to reduce the expression of many tumor promoting genes could have a global influence on the suppression of tumor development (Nasser *et al.* 2008; Datta *et al.* 2008; Yan *et al.* 2009; Reid *et al.* 2012).

Our data suggest that *Bag4* may also be a target of *miR-1* which is a novel finding. Like Ets1 and Met, Bag4 has been shown to have transforming properties (Yang *et al.* 2010). Bag4 is a member of a family of proteins that act as co-chaperones for anti-apoptotic proteins Bcl-2 and Hsp70 (Doong *et al.* 2002). The literature describing the role of BAG4 in apoptosis is mixed as BAG4 is associated with apoptosis in some studies, but appears to be anti-apoptotic in others (Ozawa *et al.* 2000; Annunziata *et al.* 2007). Additional studies are warranted to further evaluate Bag4 as a *miR-1* target and any role it may have in cSCC.

There are some limitations to this study. Only one of the three significantly differentially expressed miRNAs by qPCR was the subject of further phenotypic studies. *miR-133a* and *miR-206* may play important roles individually or in combination with *miR-1* in the

development of cSCC which were not evaluated in this study. Another weakness of this study was that candidate targets of *miRNA-1* were chosen based on the literature and predicted *in silico* screens rather than experimentally. Thus, we may have missed critical tumor suppressing targets of *miR-1* through this approach.

We identified and validated five miRNAs showing differential expression between cancer resistant and cancer susceptible mice. The mice used in the study are inbred, are age and sex-matched, and should show very similar expression profiles between mice within a strain, but it is possible that the inclusion of additional mice in the study would have led to increased power and the identification of additional miRNAs of interest. In addition, as we used a 2-fold difference in expression as our cutoff more miRNAs may show more modest differences in expression between Spret/EiJ and FVB/NJ. Nonetheless, these data are consistent with a study measuring miRNA expression of 577 miRNAs from livers of 70 different strains of inbred mice which found few to no differences in expression of any of these miRNAs (Gatti *et al.* 2011). A few studies have looked at miRNA expression in human cSCCs, but none of the miRNAs identified in those studies overlap with the ones identified here (Dziunycz *et al.* 2010).

It is interesting to note that in our original analysis, we identified miRNAs for which the precursor, but not the mature form of the miRNA showed differential expression on the array. The discrepancy may reflect transcription differences between the strains followed by miRNA processing resulting in similar amounts of mature miRNA being produced, or the precursor miRNAs may also be processed into different forms of

570 mature miRNAs, such as 5p and 3p forms, for which there were not probes on the
571 array. These data may be a reflection of our study being statistically underpowered to
572 detect some of the differences in miRNA expression. For example, *miR-206* showed
573 statistical differences in expression of the precursor miRNA but not the mature miRNA
574 by microarray, but by qPCR both the precursor and mature *miR-206* showed very
575 similar differences in expression between FVB/NJ and SPRET/EiJ.

576
577 In summary, we identified five miRNAs that show differences in expression of skin
578 between cancer resistant and cancer susceptible mice. We show evidence that *miR-1*
579 expression is decreased in cSCCs and that its expression *in vitro* leads to decreased
580 proliferation of cSCC cell lines, increased apoptosis and modest effects on cell cycle. In
581 cell lines, *miR-1* expression is correlated with decreased *Met1* and *Bag4* expression
582 and directly targets the oncogene *Ets1*. This is the first study to show that mouse *Ets1*,
583 like the human *ETS1* gene, is targeted by *miR-1*. Our studies showing similar *miR-1*
584 targets between the mouse and human suggest that mouse models of *miR-1* may be
585 useful in elucidating the role of *miR-1* in cancer. As the endogenous expression of *miR-*
586 *1* differs between skin cancer susceptible and cancer resistant mice, it may play a role
587 in the differences in cancer risk observed in these strains, but the exact mechanism
588 remains to be elucidated.

591 Funding

This work was supported in part by the American Cancer Society [RSG-07-083-01-MGO], the National Institutes of Health [CA134461] and the OSU Comprehensive Cancer Center. DG was supported by a Pelotonia Fellowship, and JF by an Up on the Roof Fellowship.

Acknowledgements

We thank John Hagan for his assistance in analysis of the microarray data and Hee-Yeon Cho for help in validation of microRNA expression profiles. Dr. Michael Ostrowski provided the *Ets1* expression construct and the Ets1 antibody. Dr. Allan Balmain provided the A5, B9 and C5N cell lines and mouse cSCC RNA. The OSU Comprehensive Microarray Shared Resource performed the miRNA expression arrays, FACS analysis was performed in the OSU Flow Cytometry Shared Resource, and the qPCR plates were run in the OSU Comprehensive Cancer Center Nucleic Acids Shared Resource.

References

- Annunziata CM, Kleinberg L, Davidson B, Berner A, Gius D, Tchabo N, Steinberg SM, Kohn EC. 2007. BAG-4/SODD and associated antiapoptotic proteins are linked to aggressiveness of epithelial ovarian cancer. *Clin Cancer Res.* 13: 6585-6592.
- Beta D, Wilson M, Gabow A, Marks DS, Sanders C. 2008. The microRNA.org resource: targets and expression. *Nucleic Acids Research*, 36: D149-D153.

- 614 Chen JF, Mandel EM, Thomson JM, Wu Q, Callis TE, Hammond SM, Conlon FL, Wang,
615 DZ. 2006. The role of microRNA-1 and microRNA-133 in skeletal muscle proliferation
616 and differentiation. *Nature Genetics*. 38: 228-233.
- 617 Childs G, Fazzari M, Kung G, Kawachi N, Brandwein-Gensler M, McLemore M, Chen Q,
618 Burk RD, Smith RV, Prystowsky MB, Belbin TJ, Schlecht NF. 2009. Low-level
619 expression of microRNAs let-7d and miR-205 are prognostic markers of head and neck
620 squamous cell carcinoma. *American Journal of Pathology*. 174: 736-745.
- 621 Ciardiello F, Tortora G. 2008. EGFR antagonists in cancer treatment. *New England*
622 *Journal of Medicine*. 358: 1160-1174.
- 623 Croce CM. 2009. Causes and consequences of microRNA dysregulation in cancer.
624 *Nature Reviews in Genetics*. 10: 704-714.
- 625 Darido C, Georgy SR, Wilanowski T, Dworkin S, Auden A, Zhao Q, Rank G, Srivastava
626 S, Finlay MJ, Papenfuss AT, Pandolfi PP, Pearson RB, Jane SM. 2011. Targeting of the
627 tumor suppressor GRHL3 by a miR-21-dependent proto-oncogenic network results in
628 PTEN loss and tumorigenesis. *Cancer Cell*. 20: 635-648.
- 629 Datta J, Kutay H, Nasser MW, Nuovo GJ, Wang B, Majumder S, Liu CG, Volinia S,
630 Croce CM, Schmittgen TD, Ghoshal K, Jacob ST. 2008. Methylation mediated silencing
631 of MicroRNA-1 gene and its role in hepatocellular carcinogenesis. *Cancer Research*.
632 68: 5049-5058.

- Dejager L, Libert C, Montagutelli X. 2009. Thirty years of Mus SPRETus: a promising future. *Trends in Genetics*. 25: 234-241.
- Dittmer J. 2003. The biology of the Ets1 proto-oncogene. *Molecular Cancer*. 2: 29.
- Doong H, Vralias A, Kohn EC. 2002. What's in the 'BAG'?—A functional domain analysis of the BAG family proteins. *Cancer Lett*. 188: 25-32.
- Djuranovic S, Nahvi A, Green A. 2011. A parsimonious model for gene regulation by miRNAs. *Science*. 331: 550-553.
- Dziunycz P, Iotzova-Weiss G, Eloranta JJ, Lauchli S, Hafner J, French LE, Hofbauer G.F.L. 2010. Squamous cell carcinoma of the skin shows a distinct microRNA profile modulated by UV radiation. *Journal of Investigative Dermatology*. 130: 2686-2689.
- Gatti DM, Lu L, Williams RW, Sun W, Wright FA, Threadgill DW, Rusyn, I. 2011. MicroRNA expression in the livers of inbred mice. *Mutation Research*. 714: 126-133.
- Gordon A, Glazko G, Qiu X, Yakovlev A. 2007. Control of the mean number of false discoveries, Bonferroni and stability of multiple testing. *The Annals of Applied Statistics*. 1: 179-190.
- Hahne JC, Okuducu AF, Kaminski A, Florin A, Soncin F, Wernert, N. 2005. Ets-1 expression promotes epithelial cell transformation by inducing migration, invasion, and anchorage-independent growth. *Oncogene*. 24: 5384-5388.

- 651 Hahne JC, Kummer S, Heukamp LC, Fuchs T, Gun M, Langer B, Von Ruecker A,
652 Wernert N, 2009. Regulation of protein tyrosine kinases in tumour cells by the
653 transcription factor Ets-1. *International Journal of Oncology*. 35: 989-996.
- 654 Huang H, Eversley CD, Threadgill DW, Zou F. 2007. Bayesian multiple quantitative trait
655 loci mapping for complex traits using markers of the entire genome. *Genetics*. 176:
656 2529-2540.
- 657 Hudson RS, Yi M, Esposito D, Watkins SK, Hurwitz AA, Yfantis HG, Lee DH, Borin JF,
658 Naslund MJ, Alexander RB, Dorsey TH, Stephens RM, Croce CM, Ambros S. 2012.
659 MicroRNA-1 is a candidate tumor suppressor and prognostic marker in human prostate
660 cancer. *Nucleic Acids Research*. 40: 3689-3703.
- 661 Kawakami K, Enokida H, Chiyomaru T, Tatarano S, Yoshino H, Kagara I, Gotanda T,
662 Tachiwada T, Nishiyama K, Nohata N, Seki N, Nakagawa M. 2012. The functional
663 significance of miR-1 and miR-133a in renal cell carcinoma. *European Journal of*
664 *Cancer*. 4: 827-836.
- 665 Keehn CA, Smoller BR, Morgan MB. 2004. Ets-1 immunohistochemical expression in
666 non-melanoma skin cancer. *Journal of Cutaneous Pathology*. 31: 8-13.
- 667 Knight ZA, Lin H, Shokat KM. 2010. Targeting the cancer kinome through
668 polypharmacology. *Nature Reviews in Cancer*. 10: 130-137.

- 669 Li D, Yang P, Li H, Cheng P, Zhang L, Wei D, Su X, Peng J, Gao H, Tan Y, Zhao Z, Li
670 Y, Qi Z, Rui Y, Zhang T. (2012). MicroRNA-1 inhibits proliferation of hepatocarcinoma
671 cells by targeting endothelin-1. *Life Sci.* 91: 440-447.
- 672 Liu CG, Calin GA, Meloon B, Gamliel N, Sevignani C, Ferracin M, Dumitru CD, Shimizu
673 M, Zupo S, Dono M, Alder H, Bullrich F, Negrini M, Croce CM. 2004. An oligonucleotide
674 microchip for genomewide microRNA profiling in human and mouse tissues.
675 *Proceedings of the National Academy of Sciences of the United States of America.* 101:
676 9740-9744.
- 677 Liu CG, Calin GA, Volinia S, Croce CM. 2008. MicroRNA expression profiling using
678 microarrays. *Nature Protocols.* 3: 563-578.
- 679 Manenti G, Gariboldi M, Elango R, Fiorino A, De Gregorio L, Falvella FS, Hunter K,
680 Housman D, Pierotti MA, Dragani TA. 1996. Genetic mapping of a pulmonary adenoma
681 resistance (Par1) in mouse. *Nature Genetics.* 12: 455-457.
- 682 McCarthy JJ. 2008. MicroRNA-206: the skeletal muscle-specific myomiR. *Biochimica et*
683 *Biophysica Acta.* 1779: 682-691.
- 684 Medina PP, Slack FJ. 2008. microRNAs and cancer: an overview. *Cell Cycle.* 7: 2485-
685 2492.
- 686 Montagut C, Settleman J. 2009. Targeting the RAF-MEK-ERK pathway in cancer
687 therapy. *Cancer Letters.* 283: 125-134.

- 688 Nagarajan P, Parikh N, Garrett-Sinha LA, Sinha S. 2009. Ets1 induces dysplastic
689 changes when expressed in terminally-differentiating squamous cell epidermal cells.
690 *PLoS One*: 4: e4179.
- 691 Nagase H, Bryson S, Cordell H, Kemp CJ, Fee F, Balmain A. 1995. Distinct genetic loci
692 control development of benign and malignant skin tumors in mice. *Nature Genetics*. 10:
693 424-429.
- 694 Nasser MW, Datta J, Nuovo G, Kutay H, Motiwala T, Majumder S, Wang B, Suster S,
695 Jacob ST, Ghoshal K. 2008. Down-regulation of micro-RNA-1 (miR-1) in lung cancer.
696 Suppression of tumorigenic property of lung cancer cells and their sensitization to
697 doxorubicin-induced apoptosis by miR-1. *Journal of Biological Chemistry*. 283: 33394-
698 33405.
- 699 Nohata N, Hanazawa T, Kikkawa N, Sakurai D, Sasaki K, Chiyomaru T, Kawakami K,
700 Yoshino H, Enokida H, Nakagawa M, Okamoto Y, Seki N. 2011. Identification of novel
701 molecular targets regulated by tumor suppressive miR-1/miR-133a in maxillary sinus
702 squamous cell carcinoma. *International Journal of Oncology*. 39: 1099-1107.
- 703 Nohata N, Sone, Y, Hanazawa T, Fuse M, Kikkawa N, Yoshino H, Chiyomaru T,
704 Kawakami K, Enokida H, Nakagawa M, Shozu M, Okamoto Y, Seki, N. 2012a. miR-1 as
705 a tumor suppressive microRNA targeting TAGLN2 in head and neck squamous cell
706 carcinoma. *Oncotarget*. 2: 29-44.

- 707 Nohata, N, Hanazawa T, Enokida H, Seki N. 2012b. MicroRNA-1/133a and microRNA-
708 206/133b clusters: dysregulation and functional roles in human cancers. *Oncotarget*. 3:
709 9-21.
- 710 Ozawa F, Friess H, Zimmerman A, Kleef J, Buchler MW. 2000. Enhanced expression of
711 silencer of death domains (SODD/BAG-4) in pancreatic cancer. *Biochem Biophys Res*
712 *Commun* 271: 409-413.
- 713 Pande P, Mathur M, Shukla NK, Ralhan R. 1999. Ets-1: a plausible marker of invasive
714 potential and lymph node metastasis in human oral squamous cell carcinomas. *Journal*
715 *of Pathology*. 189: 40-45.
- 716 Pomerantz MM, Ahmadiyeh N, Jia L, Herman P, Verzi MP, Doddapaneni H, Beckwith
717 CA, Chan JA, Hills A, Davis M, Yao K, Kehoe SM, Lenz HJ, Haiman CA, Yan C,
718 Henderson BE, Frenkel B, Barretina J, Bass A, Tabernero J, Baselga J, Regan MM,
719 Manak JR, Shivdasani R, Coetzee GA, Freedman ML. 2009. The 8q24 cancer risk
720 variant rs6983267 shows long-range interaction with MYC in colorectal cancer. *Nat*
721 *Genet*. 41: 882-884.
- 722 Quigley DA, To MD, Perez-Losada J, Pelorosso FG, Mao JH, Nagase H, Ginzinger DG,
723 Balmain A. 2009. Genetic architecture of mouse skin inflammation and tumour
724 susceptibility. *Nature*. 458: 505-508.
- 725 Reid JF, Sokolova V, Zoni E, Lampis A, Pizzamiglio S, Bertan C, Zanutto S, Perrone F,
726 Camerini T, Gallino G, Verderio P, Leo E, Pilotti S. 2012. miRNA profiling in colorectal

- 727 cancer highlights miR-1 involvement in MET-dependent proliferation. *Molecular Cancer*
728 *Research*. 10: 504-515.
- 729 Roberts PJ, Der CJ. 2007. Targeting the Raf-MEK-ERK mitogen-activated protein
730 kinase cascade for the treatment of cancer. *Oncogene*. 26: 3291-3310.
- 731 Saeki H, Kuwano H, Kawaguchi H, Ohno S, Sugimachi K. 2000. Expression of Ets-1
732 transcription factor is correlated with penetrating tumor progression in patients with
733 squamous cell carcinoma of the esophagus. *Cancer*. 89: 1670-1676.
- 734 Saeki H, Oda S, Kawaguchi H, Ohno S, Kuwano H, Maehara Y, Sugimachi K. 2002.
735 Concurrent overexpression of Ets-1 and c-Met correlates with a phenotype of high
736 cellular motility in human esophageal cancer. *International Journal of Cancer*. 98: 8-13.
- 737 Sevignani C, Calin GA, Ntadi SC, Shimizu M, Davuluri RV, Hyslop T, Demant P, Croce
738 CM, Siracusa LD. 2007. MicroRNA genes are frequently located near mouse cancer
739 susceptibility loci. *Proceedings of the National Academy of Sciences of the United*
740 *States of America*. 104: 8017-8022.
- 741 Shyu AB, Wilkinson MF, van Hoof A. 2008. Messenger RNA regulation: to translate or
742 to degrade. *The EMBO Journal*. 27: 471-481.
- 743 Siomi H, Siomi MC. 2010. Posttranscriptional regulation of microRNA biogenesis in
744 animals. *Molecular Cell*. 38: 323-332.

- Smith AM, Findlay VJ, Bandurraga SG, Kistner-Griffin E, Spruill LS, Liu A, Golshayan AR, Turner DP. 2012. ETS1 transcriptional activity is increased in advanced prostate cancer and promotes the castrate-resistant phenotype. *Carcinogenesis*. 33: 572-580.
- Spain SL, Carvajal-Carmona LG, Howarth KM, Jones AM, Su Z, Cazier JB, Williams J, Aaltonen LA, Pharoah P, Kerr DJ, Cheadle J, Li L, Casey G, Vodicka P, Sieber O, Lipton L, Gibbs P, Martin NG, Montgomery GW, Young J, Baird PN, Morreau H, van Wezel T, Ruiz-Ponte C, Fernandez-Rozadilla C, Carracedo A, Castells A, Castellvi-Bel S, Dunlop M, Houlston RS, Tomlinson IP. 2012. Refinement of the associations between risk of colorectal cancer and polymorphisms on chromosomes 1q41 and 12q13.13. *Hum Mol Genetics*. 15: 934-946.
- Tang Y, Zheng J, Sun Y, Wu Z, Liu Z, Huang G. 2009. MicroRNA-1 regulated cardiomyocyte apoptosis by targeting Bcl-2. *International Heart Journal*. 50: 377-387.
- Tominaga E, Yuasa K, Shimazaki S, Hijikata T. 2013. MicroRNA-1 targets Slug and endows lung cancer A549 cells with epithelial and anti-tumorigenic properties. *Exp Cell Res*. 319: 77-88.
- Villa-Morales M, Santos J, Fernandez-Piqueras J. 2006. Functional Fas (Cd95/Apo-1) promoter polymorphisms in inbred mouse strains exhibiting different susceptibility to gamma-radiation-induced thymic lymphoma. *Oncogene*. 25: 2022-2029.
- Wei W, Hu Z, Fu H, Tie Y, Zhang H, Wu Y, Zheng X. 2012. MicroRNA-1 and microRNA-499 downregulate the expression of the ets1 proto-oncogene in HepG2 cells. *Oncology Reports*. 28: 701-706.

- Wery M, Kwapisz M, Morillon A. 2011. Noncoding RNAs in gene regulation. *Wiley Interdisciplinary Reviews: Systems Biology and Medicine*. 3: 728-738.
- Yamasaki T, Yoshino H, Enokkida H, Hidaka H, Chiyomaru T, Nohata N, Kinoshita T, Fuse M, Seki N, Nakagawa M. 2012. Novel molecular targets regulated by tumor suppressors microRNA-1 and microRNA-133a in bladder cancer. *Int J Oncol*. 40: 1821-1830.
- Yan D, Dong Xda E, Chen X, Wang L, Lu C, Wang J, Qu J, Tu L. 2009. MicroRNA-1/206 targets c-Met and inhibits rhabdomyosarcoma development. *Journal of Biological Chemistry*. 284: 29596-29604.
- Yang ZQ, Liu G, Bollig-Fischer A, Giroux CN, Ethier SP. 2010. Transforming properties of 8p11-12 amplified genes in human breast cancer. 70: 8487-8497.
- Yoshino H, Enokida H, Chiyomaru T, Tatarano S, Hidaka H, Yamasaki T, Gotannda T, Tachiwada T, Nohata N, Yamane T, Seki N, Nakagawa M. 2012. Tumor suppressive microRNA-1 mediated novel apoptosis pathways through direct inhibition of splicing factor serine/arginine-rich 9 (SRSF9/SRp30c) in bladder cancer. *Biochem Biophys Res Commun*. 417: 588-593.
- Yu L, Gulati P, Fernandez S, Pennell M, Kirschner L, Jarjoura D. 2011. Fully moderated t-statistic for small sample size gene expression arrays. *Statistical Applications in Genetics and Molecular Biology*. 10: article42.

785 Yu XY, Song YH, Geng YJ, Lin QX, Shan ZX, Lin SG, Li Y. 2008. Glucose induced
786 apoptosis of cardiomyocytes via microRNA-1 and IGF-1. *Biochemical and Biophysical*
787 *Research Communications*. 376:548-552.

788 Zoumpourlis V, Solakidi S, Papthoma A, Papaevangeliou D. 2003. Alterations in signal
789 transduction pathways implicated in tumour progression during multistage mouse skin
790 carcinogenesis. *Carcinogenesis*. 24: 1159-1163.

791

792

793

FIGURE LEGENDS

Fig. 1. Validation of candidate miRNA expression patterns in the skin by qPCR. miRNA expression was measured by qPCR. miRNA expression in SPRET/EiJ skin (gray) relative to FVB skin (black) for five miRNAs are shown. Expression was normalized to *sno-202* for the mature miRNAs and to *L19* for the precursor RNAs. Fold expression was calculated relative to FVB/NJ. (A) *miR-1*, (B) *miR-133a*, (C) *miR-124a*, (D) *miR-206* mature, (E) *miR-206* pri, (F) *miR-134* pri (M, mature, pri-precursor. Error bars represent standard deviation. *, p-values for significance are shown for those microRNAs demonstrating p-values <0.05 for differences in miRNA expression between FVB/NJ and SPRET/EiJ.

Fig. 2. Decreased *miR-1* expression in cSCCs. *miR-1* expression was measured in eleven mouse cSCCs and six normal mouse skin RNA samples (3 FVB/NJ and 3 SPRET/EiJ) by qPCR relative to control gene *sno-202*. Median expression for each group is indicated by a line. p-value for significance between the tumors and SPRET/EiJ is indicated and was calculated using a nonparametric Mann-Whitney U test.

Fig. 3. Validation of candidate *miR-1* target genes by qPCR. Fold mRNA expression of predicted targets of *miR-1* (A) *Met*, (B) *Ets1*, (C) *Twf1* and (D) *Bag4* were assessed by qPCR. Expression is plotted as a fold difference in expression compared to the 48 hour SC transfected cells. Expression was normalized to control gene *L19*. A5 cells transfected with a scrambled control miR (SC) are shown in black and A5 cells transfected with *miR-1* are shown in gray. Cells were harvested at 48 and 72 hours

post-transfection. Difference in expression was measured by student's T-test. Error bars represent standard deviation. *, p-value < 0.01, **, p-value < 0.001.

Fig. 4. Evaluation of Ets1 as a *miR-1* target. Western blot analysis of Ets1 expression (A) 72 hours after transient transfection of A5 cells with scrambled control miR (SC) or *miR-1* and (B) 48 hours after transient transfection of B9 cells with (SC) or *miR-1*. α -tubulin (A5) or Gapdh (B9) was used as a loading control. (C) Wild type (Ets1 3'UTR) and mutated (Ets1 3'UTR SDM) Ets1 3'UTR luciferase constructs were co-transfected with scrambled control miR (SC) or *miR-1* into C5N cells. Data is expressed as relative light units of firefly over renilla luciferase. (C) The mouse *Ets1* 3'UTR has three *miR-1* binding sites. Shown are the two base pairs (bold/underlined) in the seed region of each site that were mutated using site-directed mutagenesis. Error bars represent standard deviation. **, p-value < 0.01.

Fig. 5. *miR-1* reduces cell proliferation *in vitro*. An MTT cell proliferation assay was conducted using precursor miR scramble (SC) and *miR-1* transfected in (A) A5 cells and (B) B9 cells. Hours post-transfection are indicated. Relative absorbance was measured at the indicated time points. We observed significantly decreased cell proliferation in the A5 *miR-1* transfected cells at 96 hours post-transfection (p-value, < 0.0001) and for the B9 *miR-1* transfected cells at 72 hours post-transfection (p-value < 0.01). Error bars represent standard deviation. Black diamond, scrambled control miR transfected; gray square, *miR-1* transfected; *, p-value < 0.01; ***, p-value < 0.0001.

Fig. 6. Effect of *miR-1* expression on tumor phenotypes. Apoptosis in *miR-1* or scrambled control miR transfected cells (SC) was measured at 48, 72 and 96 hours by FACS analysis in (A) A5 and (B) B9 cells. The percentage of apoptotic cells staining positive for AnnexinV and propidium iodide is indicated in scrambled control (SC) (Black) and *miR-1* transfected cells (gray) for representative experiments is shown. Cell cycle parameters for SC (black) and *miR-1* transfected A5 cells (gray) were measured in A5 cells at (C) 48 hours, (E), 72 hours and (G) 96 hours and in B9 cells at (D) 48 hours, (F) 72 hours, and (H) 96 hours by staining with propidium iodide and sorting via flow cytometry. The percentage of gated cells for G0-G1, S and G2-M phases for representative experiments are indicated. There was a statistically significant difference for S-phase for the A5 cells at all three time points. Error bars represent standard deviation. *, p-value <0.05; **, p-value<0.001; NS, not significant.

Fig. 7: Effect of *miR-1* on cell motility. Cell motility for *miR-1* and scrambled control (SC) transfected A5 cells are shown for indicated time points after removal of insert at approximately (A) 48 (B) 72 hours or (C) 96 hours after transfection. Representative experiments for each time point are shown.

Supplementary Table S1

Supplemental Table S1 contains miRNA array data for three FVB/NJ, three SPRET/EiJ samples and one replicate RNA sample (FVB-A or -B and SPRET-A or B) per strain.

Supplemental Table S2

Supplemental Table S2 lists genes predicted to be targets of the validated five miRNAs.

Supplementary Figure Legends

S1: Candidate *miR-1* target genes in B9. mRNA expression of predicted targets of *miR-1* (A) *Met*, (B) *Ets1*, (C) *Twf1* and (D) *Bag4* were assessed by qPCR. B9 cells transfected with a scrambled control miR (SC) are shown in black and B9 cells transfected with *miR-1* are shown in gray. Cells were harvested at 48, 72 and 96 hours post-transfection. Expression is plotted as a fold difference in expression compared to the 48 hour SC transfected cells. Expression was normalized to control gene *L19*. Difference in expression was measured by student's T-test. Error bars represent standard deviation. *, p-value < 0.01, **, p-value < 0.001, NS, not significant.

S2: *Ets1* levels following *miR-1* transfection. (A) Western blot analysis of *Ets1* expression 24, 48 and 72 hours after transient transfection of A5 with scrambled control miR (SC) or *miR-1*. (B) Western blot analysis of *Ets1* expression 24, 48 or 96 hours after transient transfection of B9 with SC or *miR-1*. *Gapdh* (B9) was used as a loading control.

S3: AnnexinV analysis of apoptosis. Apoptosis in *miR-1* or scrambled control miR transfected cells (SC) was measured at 48, 72 and 96 hours by AnnexinV and PI staining measured by FACS analysis. Shown is a representative sample at 72 hours

883 post-transfection for the A5 (A) SC and (B) *miR-1* transfected cells and for the B9 (C)
884 SC and (D) *miR-1* transfected cells. The gating of the cells and the percentage of
885 apoptotic cells staining positive for AnnexinV, propidium iodide or both (upper right
886 quadrant) are shown.

887 **S4: FACS analysis of cell cycle.** Cell cycle parameters were measured at 96 hours
888 post-transfection for A5 (A) scrambled control miRNA (SC) and (B) *miR-1* transfected
889 cells and for B9 (C) SC and (D) *miR-1* transfected cells by staining with propidium
890 iodide and sorting via flow cytometry. The percentage of gated cells for G0-G1, S and
891 G2-M phases are indicated.

892
893 **S5: Effects of *miR-1* on cell motility.** Cell motility for *miR-1* and SC transfected B9
894 cells are shown for 0 and 8, 11, and 13 hours after removal of insert at approximately
895 (A) 48 hours (B) 72 hours, (C) or 96 hours after transfection. Representative
896 experiments for each time point are shown.

Table 1 (on next page)

miRNAs showing statistically significant differential expression by array

[#] Average fold difference across all significant probe sets. Types of probes indicate whether probes for mature (mature), precursor (prec) or both (both) showed expression differences. *Both mouse and human probe sets were included on the array. Species indicates whether probes for mouse and/or human showed expression differences. ^When multiple probes were significant, an average of the p-value for all the probes was calculated.

Table 1: miRNAs showing statistically significant differential expression by array

miRNA	Average fold difference SPRET/FVB (range)	Types of probe	Species*	# Probes	p-value^
<i>miR-1</i>	2.6 (2.52-2.84)	Both	Both	8	1.8×10^{-5}
<i>miR-124a-3</i>	3.3	Mature	Mouse	1	1.9×10^{-7}
<i>miR-133a</i>	2.8 (2.71-2.92)	Both	Both	6	5.2×10^{-6}
<i>miR-134</i>	2.3	Prec	Human	1	2.4×10^{-6}
<i>miR-206</i>	2.6	Prec	Human	1	3×10^{-7}
<i>miR-9-1</i>	2.1	Prec	Mouse	1	1.7×10^{-5}

Average fold difference across all significant probe sets. Types of probes indicate whether probes for mature (mature), precursor (prec) or both (both) showed expression differences. *Both mouse and human probe sets were included on the array. Species indicates whether probes for mouse and/or human showed expression differences. ^When multiple probes were significant, an average of the p-value for all the probes was calculated.

Figure 1

Validation of candidate miRNA expression patterns in the skin by qPCR

miRNA expression was measured by qPCR. miRNA expression in SPRET/EiJ skin (gray) relative to FVB skin (black) for five miRNAs are shown. Expression was normalized to *sno-202* for the mature miRNAs and to *L19* for the precursor RNAs. Fold expression was calculated relative to FVB/NJ. (A) *miR-1*, (B) *miR-133a*, (C) *miR-124a*, (D) *miR-206* mature, (E) *miR-206* pri, (F) *miR-134* pri (M, mature, pri-precursor. Error bars represent standard deviation. *, p-values for significance are shown for those microRNAs demonstrating p-values <0.05 for differences in miRNA expression between FVB/NJ and SPRET/EiJ.

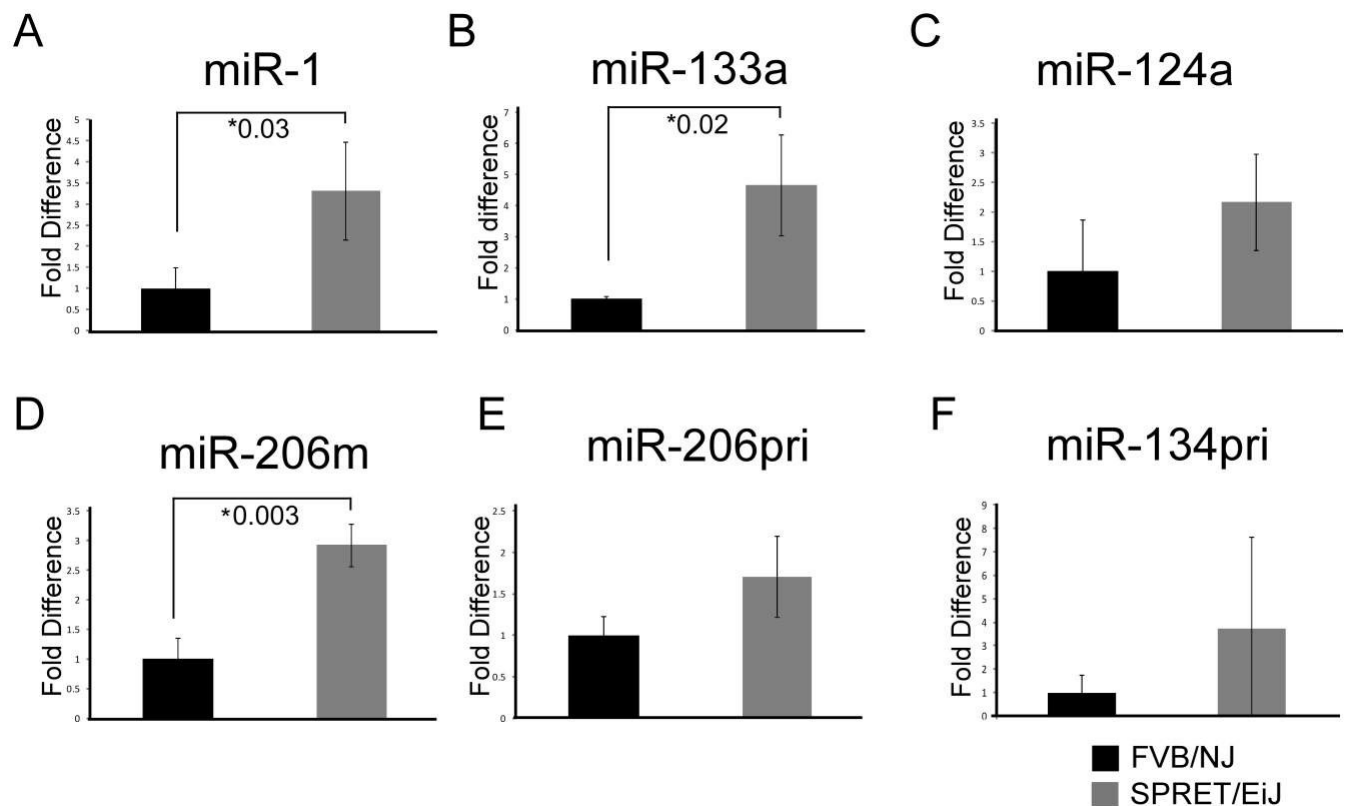


Figure 2

Decreased *miR-1* expression in cSCCs

miR-1 expression was measured in eleven mouse cSCCs and six normal mouse skin RNA samples (3 FVB/NJ and 3 SPRET/EiJ) by qPCR relative to control gene *sno-202*. Median expression for each group is indicated by a line. p-value for significance between the tumors and SPRET/EiJ is indicated and was calculated using a nonparametric Mann-Whitney U test.

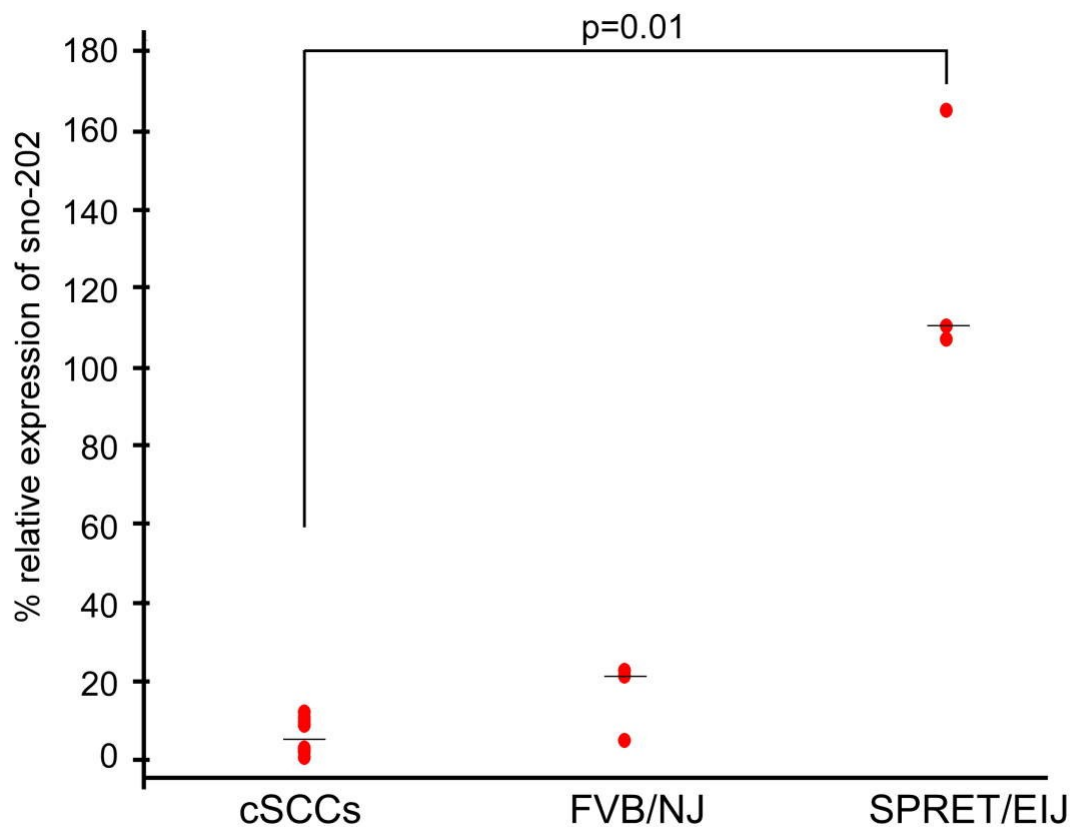


Figure 3

Validation of candidate *miR-1* target genes by qPCR

Fold mRNA expression of predicted targets of *miR-1* (A) *Met*, (B) *Ets1*, (C) *Twf1* and (D) *Bag4* were assessed by qPCR. Expression is plotted as a fold difference in expression compared to the 48 hour SC transfected cells. Expression was normalized to control gene *L19*. A5 cells transfected with a scrambled control miR (SC) are shown in black and A5 cells transfected with *miR-1* are shown in gray. Cells were harvested at 48 and 72 hours post-transfection. Difference in expression was measured by student's T-test. Error bars represent standard deviation. *, p-value < 0.01, **, p-value < 0.001.

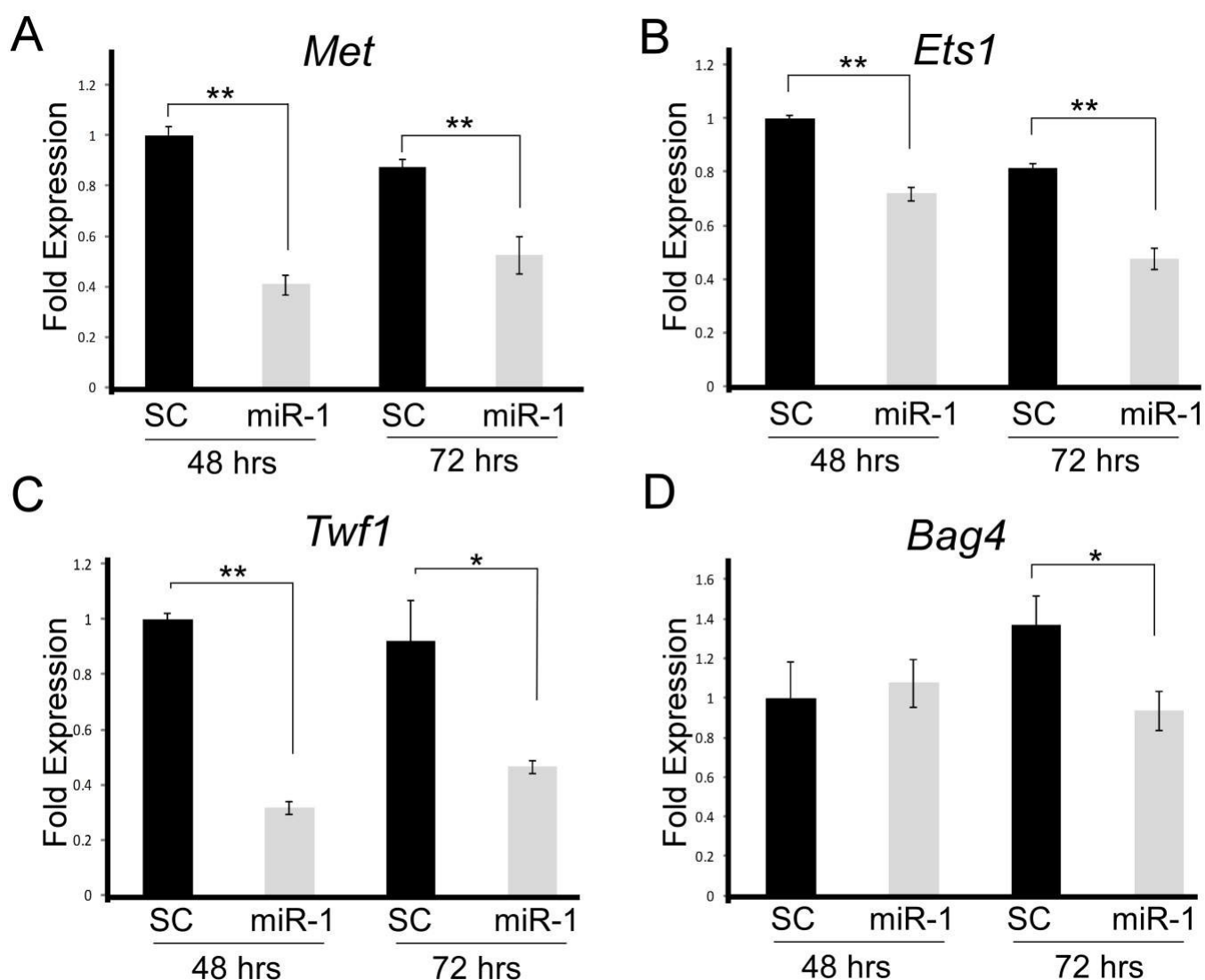


Figure 4

Evaluation of Ets1 as a *miR-1* target

Western blot analysis of Ets1 expression (A) 72 hours after transient transfection of A5 cells with scrambled control miR (SC) or *miR-1* and (B) 48 hours after transient transfection of B9 cells with (SC) or *miR-1*. alpha-tubulin (A5) or Gapdh (B9) was used as a loading control. (C) Wild type (Ets1 3'UTR) and mutated (Ets1 3'UTR SDM) Ets1 3'UTR luciferase constructs were co-transfected with scrambled control miR (SC) or *miR-1* into C5N cells. Data is expressed as relative light units of firefly over renilla luciferase. (C) The mouse *Ets1* 3'UTR has three *miR-1* binding sites. Shown are the two base pairs (bold/underlined) in the seed region of each site that were mutated using site-directed mutagenesis. Error bars represent standard deviation. **, p-value < 0.01.

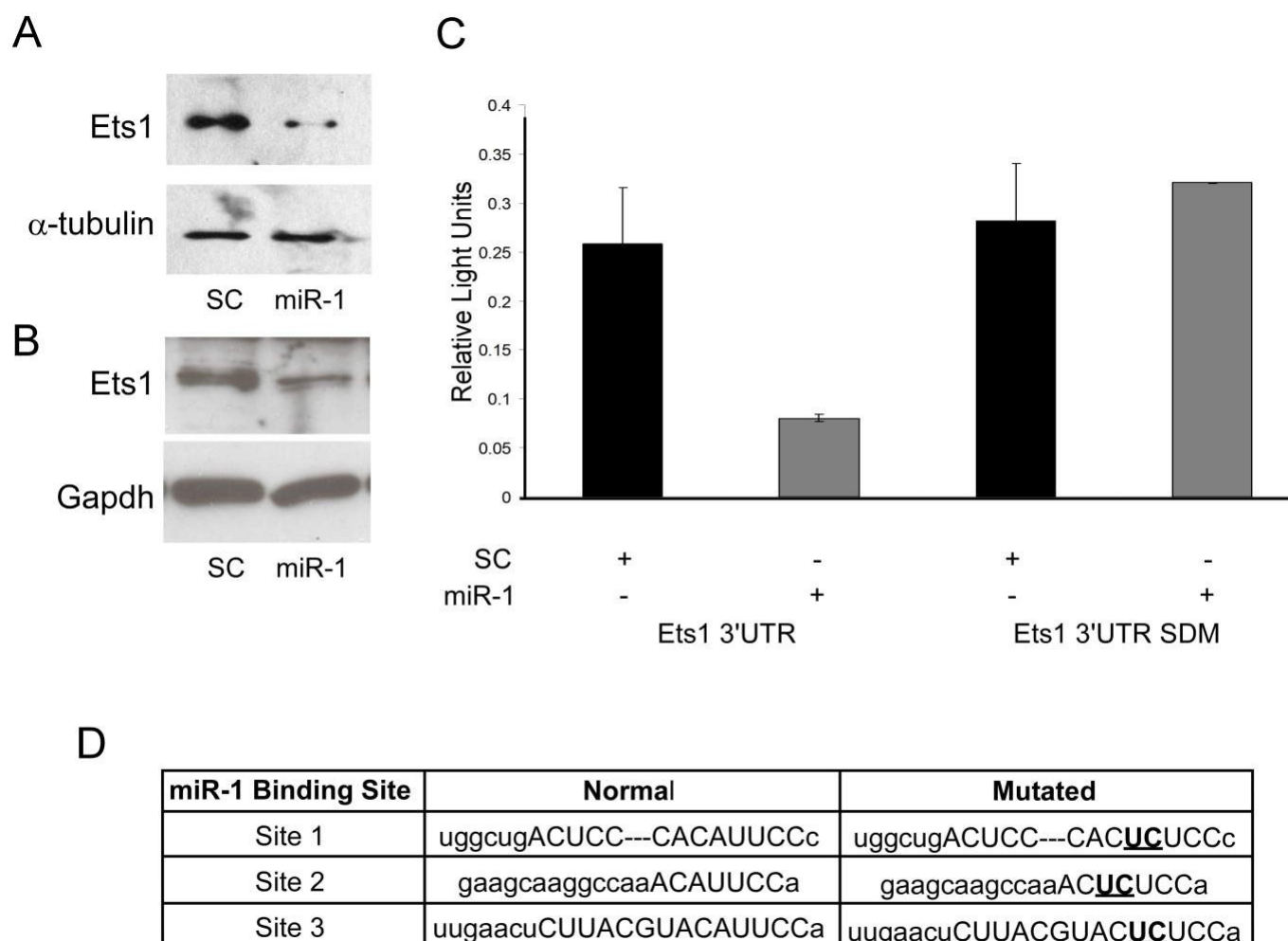
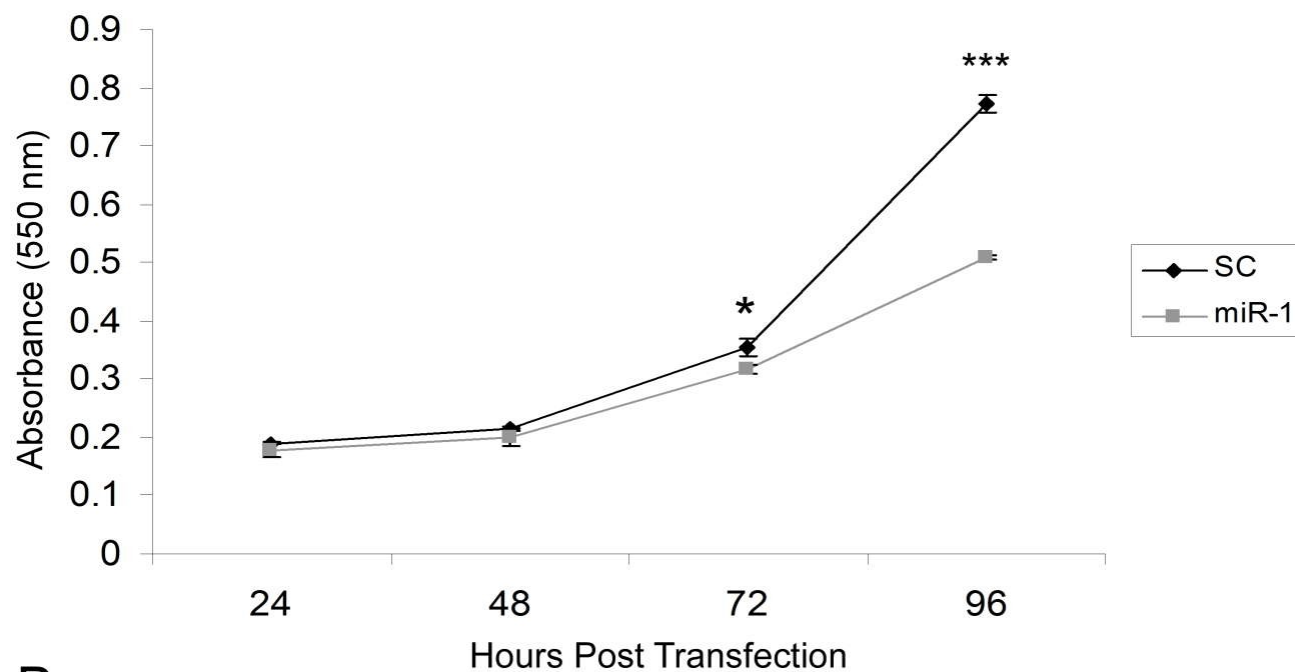


Figure 5

miR-1 reduces cell proliferation *in vitro*

An MTT cell proliferation assay was conducted using precursor miR scramble (SC) and *miR-1* transfected in (A) A5 cells and (B) B9 cells. Hours post-transfection are indicated. Relative absorbance was measured at the indicated time points. We observed significantly decreased cell proliferation in the A5 *miR-1* transfected cells at 96 hours post-transfection (p -value, < 0.0001) and for the B9 *miR-1* transfected cells at 72 hours post-transfection (p -value < 0.01). Error bars represent standard deviation. Black diamond, scrambled control miR transfected; gray square, *miR-1* transfected; *, p -value < 0.01 ; ***, p -value < 0.0001 .

A



B

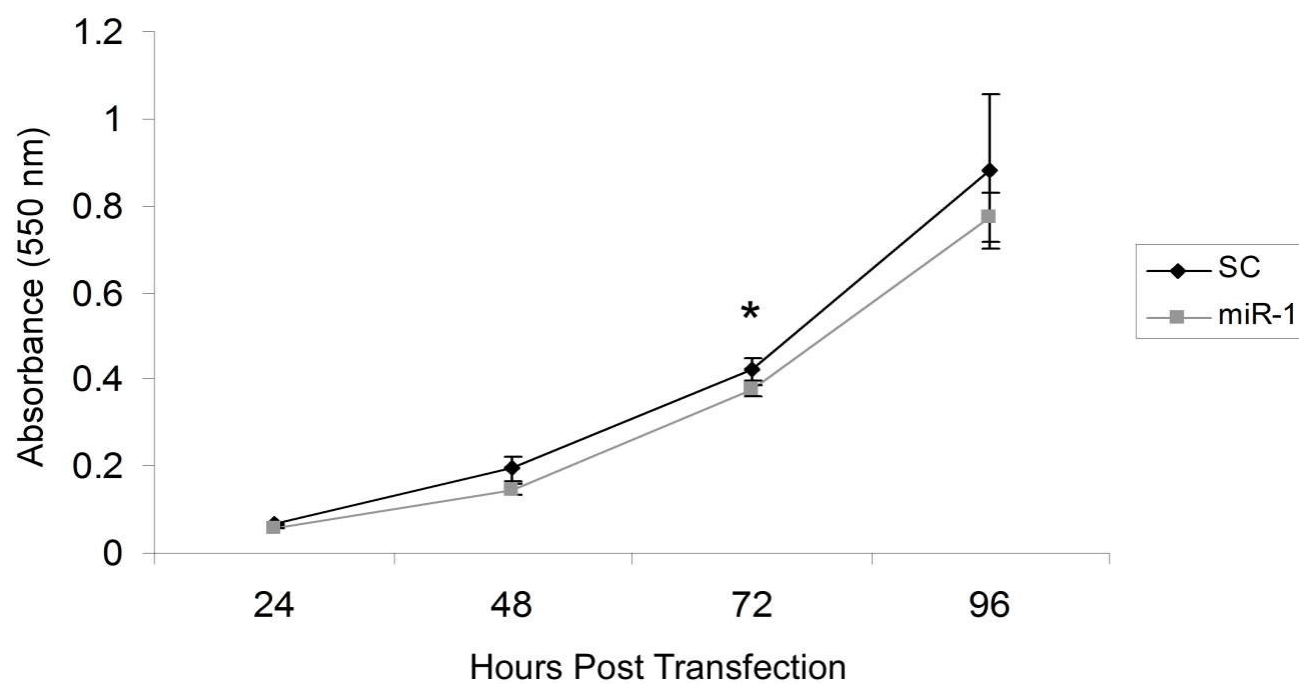


Figure 6

Effect of *miR-1* expression on tumor phenotypes

Apoptosis in *miR-1* or scrambled control miR transfected cells (SC) was measured at 48, 72 and 96 hours by FACS analysis in (A) A5 and (B) B9 cells. The percentage of apoptotic cells staining positive for AnnexinV and propidium iodide is indicated in scrambled control (SC) (Black) and *miR-1* transfected cells (gray) for representative experiments is shown. Cell cycle parameters for SC (black) and *miR-1* transfected A5 cells (gray) were measured in A5 cells at (C) 48 hours, (E), 72 hours and (G) 96 hours and in B9 cells at (D) 48 hours, (F) 72 hours, and (H) 96 hours by staining with propidium iodide and sorting via flow cytometry. The percentage of gated cells for G0-G1, S and G2-M phases for representative experiments are indicated. There was a statistically significant difference for S-phase for the A5 cells at all three time points. Error bars represent standard deviation. *, p-value <0.05; **, p-value<0.001; NS, not significant.

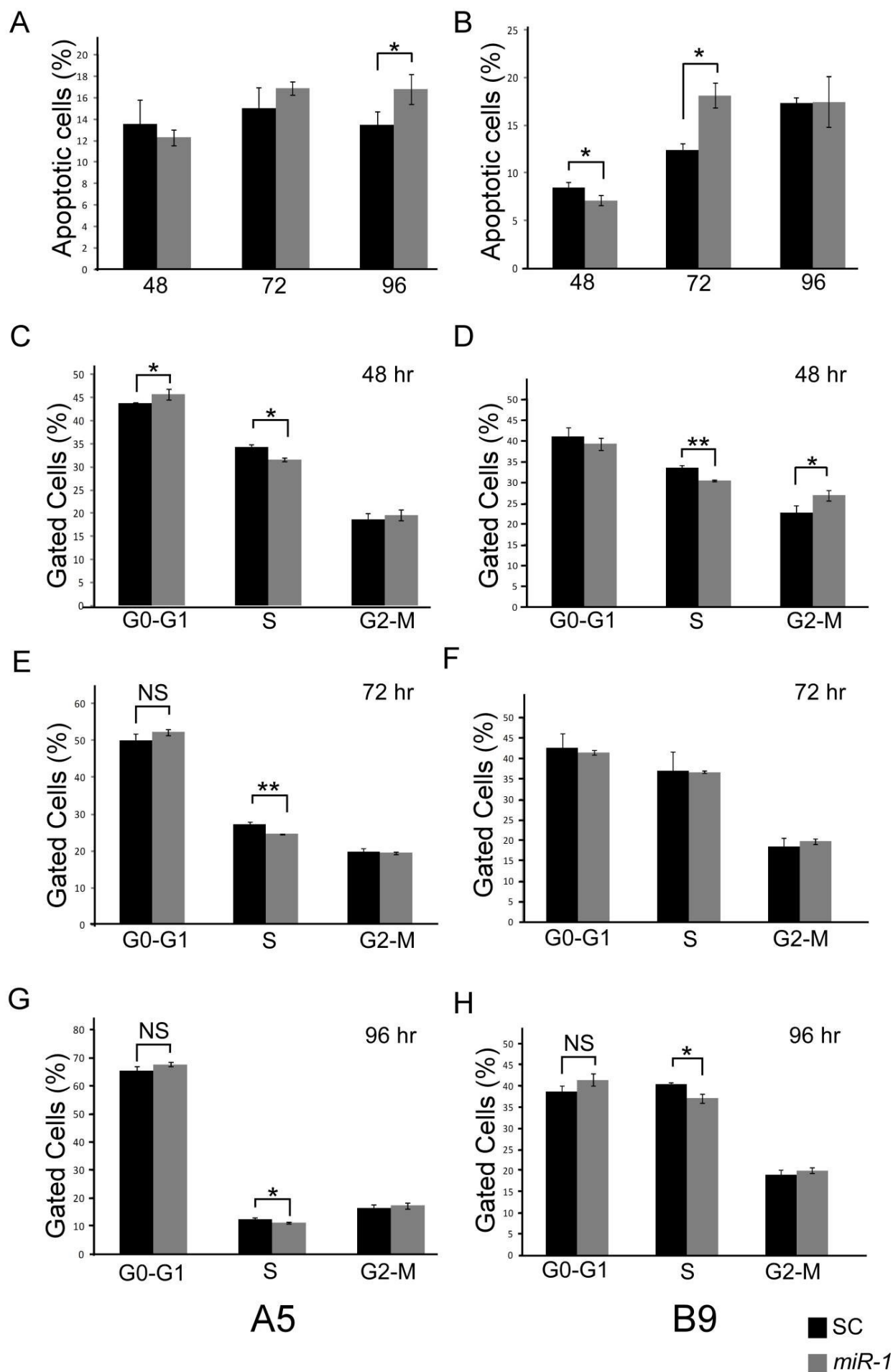


Figure 7

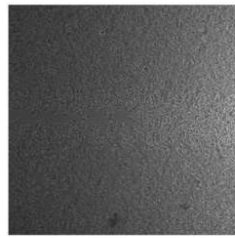
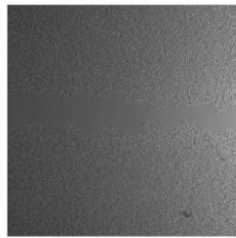
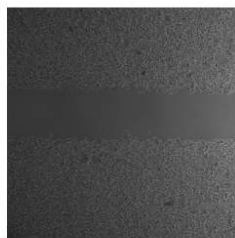
Effect of *miR-1* on cell motility

Cell motility for *miR-1* and scrambled control (SC) transfected A5 cells are shown for indicated time points after removal of insert at approximately (A) 48 (B) 72 hours or (C) 96 hours after transfection. Representative experiments for each time point are shown.

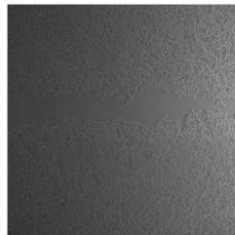
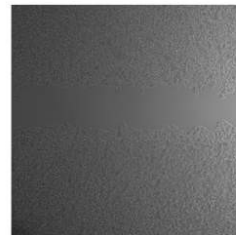
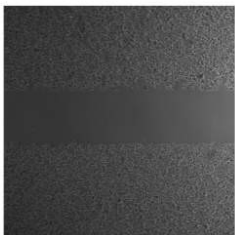
A

48 hours post-transfection

SC



miR-1



0 hours

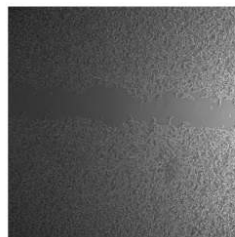
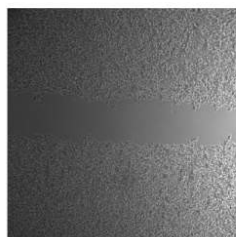
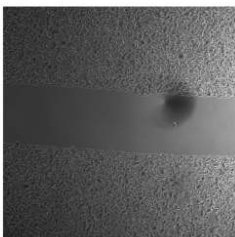
13 hours

22 hours

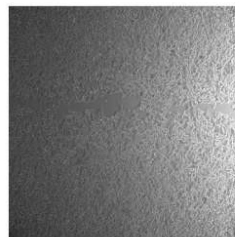
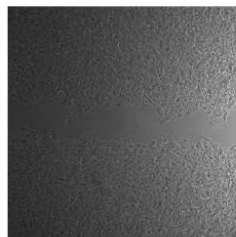
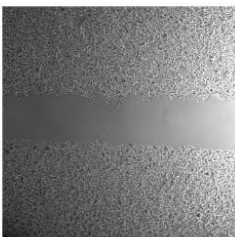
B

72 hours post-transfection

SC



miR-1



0 hours

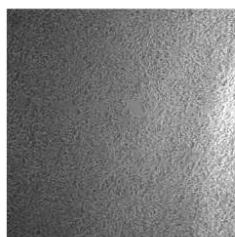
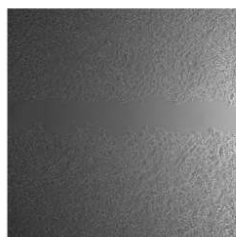
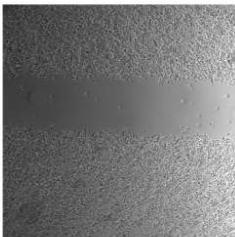
13 hours

20 hours

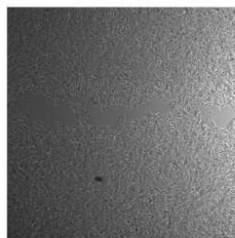
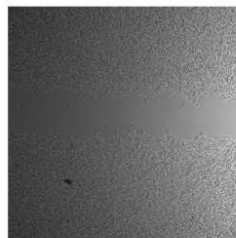
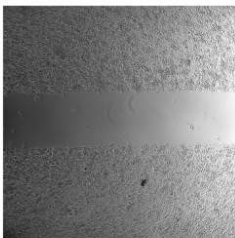
C

96 hours post-transfection

SC



miR-1



0 hours

11 hours

25 hours